April 2015

Chemical Screening and Analysis of C. albicans and P. aeruginosa in Presence of Filastatin

Kayli J. Kacoyannakis
Worcester Polytechnic Institute

Chemical Screening and Analysis of *C. albicans* and *P. aeruginosa* in Presence of Filastatin

A Major Qualifying Project

Submitted to the Faculty of the

Chemical Engineering and Biology/Biotechnology Departments

Worcester Polytechnic Institute

Worcester, MA 01609

In Partial Fulfillment of the Requirements for the

Degree of Bachelor of Science in

Chemical Engineering

and

Biology/Biotechnology

Submitted and Approved on

April 30, 2015

Kayli J. Kacoyannakis

Reeta Rao Ph.D., Project Advisor

Terri Camesano Ph.D., Project Advisor

Abstract

Candida albicans and *Pseudomonas aeruginosa* are two of the most common healthcare related diseases today. *Candida* is ranked the 4th most common cause of over 46,000 healthcare associated bloodstream infections (CDC, 2013). *Pseudomonas* causes 51,000 healthcare related infections in both the bloodstream and at surgical sites (CDC, 2013). Due to their ability to form infectious biofilms on biotic and abiotic surfaces, they are rapidly becoming antibiotic resistance over time. With very few new drugs manufactured each year, only 13 in 2014 (CDC), these infections pose serious public health threats. Alternative treatments are urgent. Filastatin is a small molecule that exhibits inhibitory properties when applied to *Candida albicans*. It is shown to inhibit the adhesion and filamentation of the fungus to abiotic surfaces. Growth phases of *C. albicans* and *P. aeruginosa* when exposed to Filastatin were examined to identify any effects on microbial formation. Results indicated that Filastatin does disrupt the initial growth of both *C. albicans* and *P. aeruginosa*.

Acknowledgements

I would like to thank Professor Reeta Rao and Professor Terri Camesano for collaborating and hosting this project. I'd also like to thank Professor Christopher Lambert for opening his lab and post-doctoral research associate to me. Lastly, I'd like to thank Dr. Aung Lynn for his help with experiments, out of the box ideas, and informative conversations.

Table of Contents

Table of Figures

Introduction

In 2013, the CDC ranked *Candida albicans* and *Pseudomonas aeruginosa* as serious antibiotic resistant threats. *Candida* is ranked the 4th most common cause of over 46,000 healthcare associated bloodstream infections (CDC, 2013). *Pseudomonas* causes 51,000 healthcare related infections in both the bloodstream and at surgical sites (CDC, 2013). From 1998-2003, a 56% decrease in new FDA approved drugs was observed (Spellberg B, 2004). In 2014, only 13 were discovered and approved. Overall, this is a growing problem as both *C. albicans* and *P. aeruginosa* are becoming resistant to the available drugs. With the small amount of new drugs reaching the market each year, this problem worsens thus the need for antifungal and antibacterial agents is urgent (Conly, 2005).

The first prevalent pathogen is *Candida albicans*, a common dimorphic fungus known to naturally live in the gastrointestinal tract, mouth, epithelial lining, and genital tract of humans without highly negative effects. As seen in *Figure 1* this fungus possesses two morphological features: oval (blastospore) and filament. The yeast form, or blastospore, of the fungus grow at low pH and typically bud off of the hyphal nodes when in pseudohyphae form (Kadosh, 2005). The filament shape can survive a variety of pH levels and are constricted by the groups of blastospores. If the fungus enters hyphae form these constrictions are absent allowing unbroken elongated cells that are predicted to be much more invasive populate (Saville, 2003). In order for the fungus to be infectious, free switching between the pseudohyphae and hyphae form is required (Saville, 2003).

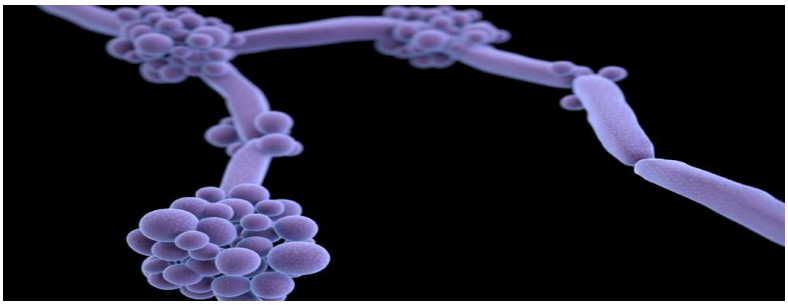

Figure 1: Commensal C. albicans Structure (CDC, 2013)

C. albicans is known to be dimorphic in that it switches between the two structures depending on environmental conditions. The transition from blastospore to filament can occur at elevated body temperatures (37°C) and in the presence of serum or certain human hormones (Kadosh, 2005). When a patient's immune system is compromised, the environment in which the fungus naturally occurs changes to a set of ideal conditions for the morphological transition. This enables *C. albicans* to more commonly undergo hyphae growth where more filament forms are made. These shapes are required for deep-seated infection as they are better suited for penetrating the mammalian host tissue but the transition in which they are formed is required for initial virulence (Liu, 2004).

This transition is known to induce 61 genes in response to higher temperature and/or presence of serum. About half of these are transcriptionally repressed when in the blastospore shape by Rfg1, Nrg1, and Tup1 (Kadosh, 2005). In order to determine if these genes that induce filament formation are the initial cause of virulence, an engineered strain containing Nrg1 and a tetracycline promoter was done in 2003. When mice were injected with the strain and exposed to the ideal conditions for blastospore-filament transition, infection and mortality was observed. When placed under normal, non-immunocompromised conditions mortality was not observed. This indicated that the morphogenetic conversion that leads to the activation of multiple genes that

leads to the growth of continuous filaments is necessary for the pathogenesis of *C. albicans* (Saville, 2003).

Not only does the morphological plasticity of this fungus pose a problem if environmental changes are common but the strongest set of hyphal transition filament that leads to virulence includes heightened body temperature and serum, such as blood (Ernst, 2000). These are common in a healthcare setting as the patient is fighting infection as well as exposed to many instruments that can come in contact with bodily fluids such as blood.

Biofilms of *C. albicans* are the most likely to come in contact with bodily fluids and further grow due to an ideal environment. The morphological plasticity of *C. albicans* also enables it to be highly resilient when a biofilm is formed. Biofilms are a large group of cells that adhere to a biotic or abiotic surface and grow to form an extracellular matrix (ECM). A biofilm can be compared to a blister where the outside is tough and protects the inside. Cell density is greatest at the base and inside of a biofilm leading to an extremely thick mass of cells embedded in the ECM as seen in *Figure 2* (Ganguly, 2011). The ECM is known to contain host immune cells called neutrophils. Neutrophils can adsorb many things including antibiotics thus preventing the lower layers of the biofilm from being harmed (Ganguly, 2011). This physical characteristic alone causes the biofilm to be nearly impenetrable (Ganguly, 2011).

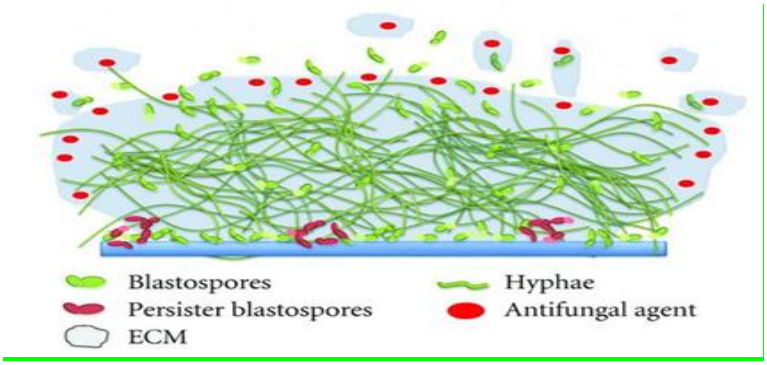

Figure 2: C. albicans Biofilm Structure (hindawi)

Not only does this complex ECM layer of a biofilm protect the inside but it produces two components that make it infectious: Farnesol and Tyrosol. Farnesol is an inhibitor of hyphal formation while Tyrosol is a stimulator. Although these two molecules counteract each other, as cell density of a biofilm increases the production of Tyrosol becomes greater than Farnesol leading to the infectious pseudohyphae-hyphae transition of the many embedded yeast and filamentous cells found in the ECM (Finkel, 2010). Thus the production of more infectious filament structures occurs (Finkel, 2010). The more a biofilm grows the thicker it becomes making it more drug resistant. The thicker it becomes the more it irreversibly adheres to the surface. The more cell density increases the more Tyrosol is produced causing it undergo the transition that makes it infectious. Because of this, biofilms pose a large problem in a medical setting as they can appear on many things such as catheters and implants that come in contact with bodily fluids (Finkel, 2010). As long as it is a solid surface, bacteria and fungus alike are able to stick to it and grow.

Not only are biofilms impenetrable, drug resistant infectious masses, but they have been shown to prevent the activation of reactive oxygen species (Xie, 2012). ROS are compounds produced by an enzyme called NADPH oxidase found in phagocytic cells. If a pathogen is recognized by the system, this complex is assembled within the phagocytic membrane and allowed to react with superoxide radicals. Once reacted, hydrogen peroxide is produced and transported into the neutrophil within the phagocyte (Edens, 2001). This creates an antibacterial or antifungal environment within the phagocyte leading to eventual cell death (Edens, 2001). Because *C. albicans* biofilms are known to reduce the production of ROS, this antimicrobial environment is no longer created thus phagocytes are no longer killed. If they are not killed they are able to recruit others and further infect a patient.

Because of these many properties, *C. albicans* is able to infect all major organs and tissues of the human body (Saville, 2003). When placed in a healthcare setting where biofilm formation is common and come in contact with an environmental niche for hyphal growth, *C. albicans* quickly becomes a well-supported newly infectious pathogen.

It is clear that *C. albicans* poses a large problem regarding medical related infections. With a 30% mortality rate related to medical devices since 2004, an antifungal solution is necessary (Kojic, 2004).

The second pathogen, *Pseudomonas aeruginosa* is said to range from 18% to 61% mortality rates with an 87.8% antibiotic resistance in 2008 (Kang, 2003; Vitkauskienė, 2011) making it another large issue in the healthcare field. This gram-negative bacteria is problematic for patients with cystic fibrosis, immunocompromised systems, and with burn injuries. Due to the structure of *P. aeruginosa* as seen in *Figure 3*, it's able to attach to a variety of surfaces and interact with the host (Ivanov, 2010).

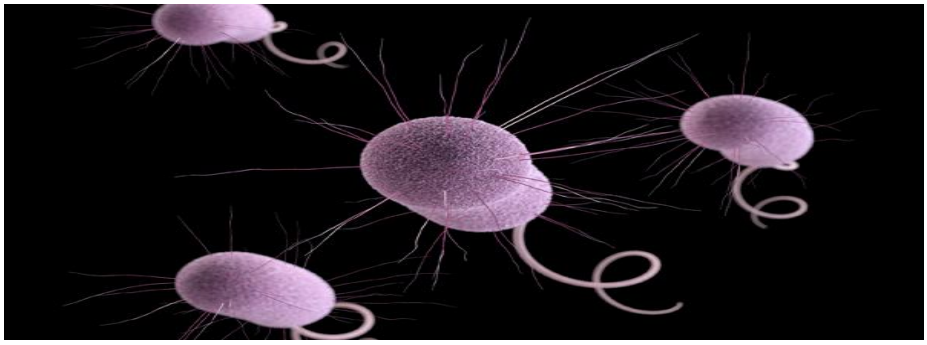

Figure 3: P. aeruginosa Structure (CDC, 2013)

Pseudomonas aeruginosa consists of lipopolysaccharides (LPS) in the outer layer of the cell. LPS contains lipid A that anchors it to the outer membrane, a core oligosaccharide, and sugar side chains such as O-antigens and H-antigens (Ivanov, 2010). The O-antigen side chain consists of repeating saccharide units that impart serospecificity and protrude into the surrounding environment as seen in *Figure 3* (Ivanov, 2010). These long side chains enable the bacteria to

interact with its surroundings and contribute to its adhesion ability (Ivanov, 2010). *P. aeruginosa* also consists of an H-antigen which is a single flagella at the base of the structure allowing it move across surfaces it may adhere to (Stanislavsky, 1997).

Although this bacteria consists of an extremely invasive physical structure, it has been shown that the O-antigen is required for virulence (Ivanov, 2010). Without the long sugar chain protruding into the environment, less adhesion to epithelial cells can occur (Tang, 1996). Similar to *C. albicans*, *P. aeruginosa* is still viable if part of its structure is missing. In *C. albicans*, filament forms are not required for viability. In *P. aeruginosa*, O-antigens are not required for viability either (Kintz, 2008).

As mentioned, it has been shown that the O-antigen is required for bacterial virulence. This is not the case regarding Cystic Fibrosis patients making this type of infection even more complicated. When a patient has cystic fibrosis, epithelial cells express a delta F508 alelle in the cystic fibrosis transmembrane conductance regulator or CFTR (Pier, 1996). This expression in CFTR causes the cells to be defective in uptake of *P. aeruginosa* as it only ingests the core-oligosaccharide (Pier, 1996). Knowing that bacterial virulence requires the uptake of the O-antigen side chain, one would think that this defect would protect the epithelial cells from infection. Instead, an increase in bacterial accumulation in the lungs of cystic fibrosis patients is observed (Pier, 1996). It is inferred that this allele expression in CFTR contributes to the virulence of *P. aeruginosa* (Pier, 1996). This interaction poses an even larger problem in the medical field as one infection is able to make another express bacterial virulence.

Patients without cystic fibrosis such as immunocompromised or burn victims have not shown these types of interactions. The O-antigen appears to still be required for bacterial virulence. Because these sugar chains consist of saccharide units, they can vary in length thus vary in

virulence (Ivanov, 2010). The longer the sugar chain, the more units can interact and bind to surrounding surfaces. It has been shown that these O-antigens can change in length depending on the surface it initially adheres to (Ivanov, 2010). Such an ability allows *P. aeruginosa* to not only interact with a variety of surfaces but effectively adhere to many of them through variation in its O-antigens (Ivanov, 2010).

Similarly to *C. albicans*, *P. aeruginosa* is able to form biofilms on various surfaces due to interactive structure. Biofilm formation depends on quorum sensing or QS between the cells on a surface such as glass. When cell density of a formation of cells is high enough, QS induces the production of acylated homoserine lactones (Schaber, 2007). When these AHLs are produced in a P. aeruginosa biofilm, they are able to bind and regulate the activity of transcription factors LasR and RhlR. These two factors are then able to transcribe multiple genes that can produce toxins that lead to the virulence of the bacterial biofilm (Schaber, 2007). Biofilm formation not only begins with antigens shown to cause virulence adhering to a surface but also increases in virulence due to a cascade effect as a result of quorum sensing (Schaber, 2007). In the medical field where biofilm formation is common, this is a large threat.

These antigens are extremely effective for the bacterial virulence, antibiotic resistance, and biofilm formation of *P. aeruginosa* but also exhibit some beneficial properties. O-antigens and the H-antigen are highly immunogenic (Stanislavsky, 1997). Among these antigens is a mucoid substance on the surface of the bacteria that contain unique epitopes. When these epitopes are found in the antigens, cross-protective immunity against *P. aeruginosa* is observed indicating a potential vaccine application (Stanislavsky, 1997). When injecting a vaccine containing these epitopes at low masses of 20 to 100kDa into human volunteers, high levels of antibodies against

P. aeruginosa were found (Stanislavsky, 1997). Plasma containing these antibodies helped recover 87% of patients with severe forms of *P. aeruginosa*.

These results indicate that not only does the structure lead the bacteria to be extremely invasive, but it can be used to treat *P. aeruginosa* as well. Because *P. aeruginosa* is a serious medically related infection (CDC, 2013), all avenues for treatment should be explored. A vaccine using the very antigen that makes it infectious has shown promising signs but the goal is to prevent the infection entirely thus the need for an antibacterial treatment is necessary.

Materials and Methods

Strains

In all experiments, the medically common strain used for *C. albicans* was CS 5314. The strain used for *P. aeruginosa* was PAO1 F173. Both strains were kindly provided by Professor Reeta Prusty Rao, Worcester Polytechnic Institute and kept at -4°C for later use. When needed, samples were taken from original supply and grown in fresh media to ensure viable cells.

Establishment of Optical Density vs. Cell Concentration Correlation

All strains were maintained in tryptic soy broth (TSB). 30 µl of *C. albicans* CS 5314 from overnight culture in TSB was added to 30 ml of fresh TSB medium in the 25 ml Falcon® tissue culture flask (Becton Dickinson, Franklin Lakes, NJ). This was incubated on a Glas-Col 099A-RD4512 Rotator (Terre Haute, IN) at 37 ˚C. 2 ml of sample from the container was taken at different time points such as 0 hour, 3 hour, 6 hour, etc. and its optical density was measured by using Evolution 300 UV-visible spectrophotometer (Thermo Scientific). The data obtained was processed using Microsoft Excel 2013 to identify a time point at which *C. albicans* growth reaches 1 O.D. at 600 nm. This process was repeated using *P. aeruginosa*. Up to three additional trials were carried out to establish data consistency.

To examine the effects of Filastatin on the growth of both C. albicans and P. aeruginosa, 12.5 µM of Filastatin was added to the same mixture described earlier. 2 ml of sample from the container was taken at different time points such as 0 hour, 3 hour, 6 hour, etc. and its optical density was measured by using Evolution 300 UV-visible spectrophotometer (Thermo Scientific). The data obtained was processed using Microsoft Excel 2013 to identify any changes in growth

time of *C. albicans* when in the presence of Filastatin. This process was repeated using *P. aeruginosa*. Up to three additional trials were carried out to establish data consistency.

To determine a cell concentration curve in reference to incubation time, 200 µl of the 2 ml samples taken during each of the four growth curves was loaded into a Bright Line® hemacytometer (Reichert, Buffalo, NY) for cell counting. Using a microscope at 40X, the four corner squares of the outside perimeter as well as center square were used to count cells. 10-fold serial dilutions using TSB were required at times if cell density was too high. An average number of cells per square taken by dividing the total by 5. By multiplying the resulting number by the dilution factor of the sample and concentration of 10^4, a final cell number per mL was determined. These results were plotted in comparison to incubation time and corresponding OD data. Because OD and cell concentration now share the same x values, a plot of OD vs. cell concentration can be made. By fitting a linear trend line to the data, a correlation equation was determined. Due to the small size and mobility of *P. aeruginosa*, it was not counted by hand using a hemacytometer. Instead a literature correlation was used (Kim, 2012). Ideally, growing the 2 ml sample taken at each time point could have been plated on Tryptic Soy Agar, incubated at 27°C overnight, and colonies hand counted.

Biofilm Growth and Bioreactor Experiment

$3x10^4$ cells/ml of *C. albicans* CS 5314 in 1L TSB was kept at 0 ˚C and was allowed to flow on (3-aminopropyl)-trimethoxylsilane (APTMS) and bare glass surfaces in the bioreactor. APTMS prevents the adsorption of small organic molecules to the glass surface while increasing the number of bonds between them (Seed, 2003). Because of this a larger amount of biofilm was expected on the APTMS coated glass coupons. The system was run using a Manostat Carter

Cassette Pump (Barnant Company, Barrington, IL) at a flow rate of 329 µL/min to simulate physiological flow. This helps represent bloodstream infections where both *C. albicans* and *P. aeruginosa* are able to spread throughout the body. Both bioreactors were then placed in a 37˚C water bath to simulate the slightly higher body temperature of an immunocompromised system that is ideal for both *C. albicans* and *P. aeruginosa* biofilm formation. The system was run for 17 hours or until the mixture was gone.

Crystal Violet Adhesion Assay Staining and Analysis

After 17 hours of incubation, glass coupons were removed from the bioreactors and stained with 0.3 ml of Gram crystal violet (Becton Dickinson, Franklin Lakes, NJ) for 15 minutes. The crystal violet stain was carefully removed using a micropipetter and the surface was rinsed gently 3 times with Phosphate-Buffered Saline to remove any extra stain. Biofilm was dissolved in 0.5 ml of 33% (v/v) acetic acid. The optical density of the dissolved biofilm was quantified using a Victor3 1420 multilabel reader (Perkin-Elmer, Waltham, MA) at 590 nm. The data obtained was processed by using Microsoft Excel 2013 to identify how much biofilm formed on each coupon. This process was repeated using *P. aeruginosa*. Data was processed using Microsoft Excel 2013 to determine the cell concentration of the biofilms formed on each coupon.

Results

Establishment of Optical Density vs. Cell Concentration Correlation

The goal of this project is to determine the effects on cell concentration of *C. albicans* and *P. aeruginosa* that Filastatin may have. To achieve this, a method for determining cell concentration is needed. Growth curves for *C. albicans*, *C. albicans* + Filastatin, *P. aeruginosa*, *P. aeruginosa* + Filastatin were established over 24 hours in Tryptic Soy Broth media.

2 ml samples were collected, an optical density reading obtained using a spectrometer, and a cell count performed using a hemacytometer. By plotting incubation time versus OD or cell concentration, growth curves of *C. albicans* could be established as seen in *Figure 14* and *Figure 15* in *Appendix A*. Using Microsoft Excel 2013, a plot of OD versus cell count could then be generated as seen in *Figure 4*. An equation relating OD and cell concentration could then be found by fitting a linear trend line to the data. Summary tables of calculations relating to *Figure 14* and *Figure 15* can be found in the *Appendix B*. Multiple trials were performed to ensure consistent results.

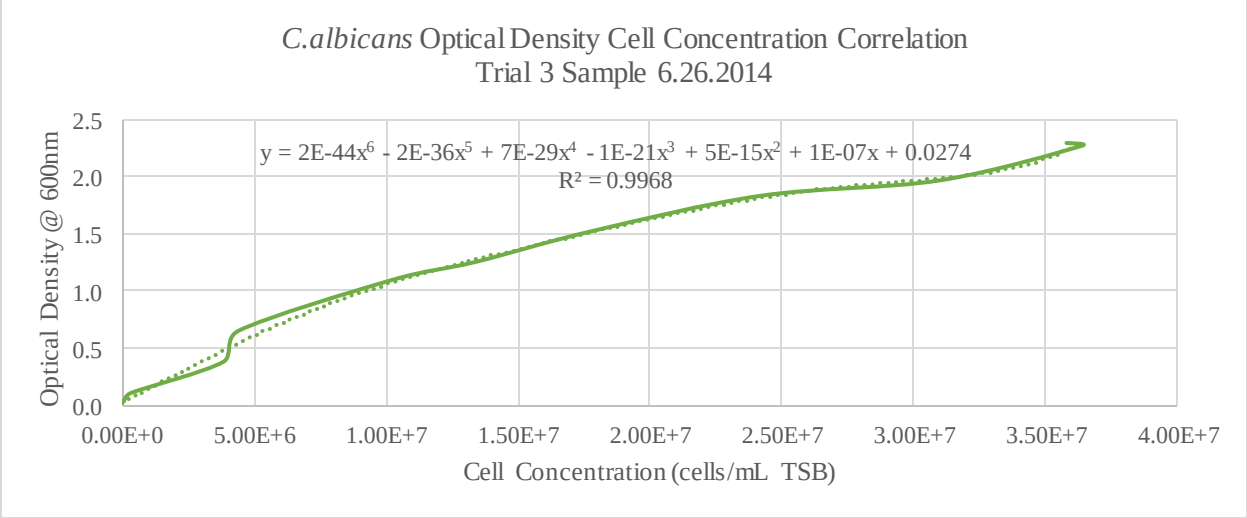

Figure 4: C. albicans OD at 600nm vs. Cell Concentration in cells/ml

Optical density for *P. aeruginosa* was determined using the same process as for *C. albicans* and plotted in *Figure 16* in *Appendix A*. Cell concentration could not be determined using the cell counting and hemacytometer method. Due to the mobility and morphological properties of this bacteria, it was impossible to count the number of cells in each time sample using a hemacytometer. A flow cytometer could not be used either as the flagella tail on *P. aeruginosa* allows it to move in all directions. This would cause the flow cytometer to potentially read the same cell twice if it were to move in the reverse direction past the sensor. A literature correlation for optical density versus cell concentration was found instead (Kim, 2012). In this technique they plated 100 µl of samples taken at various time points, grew them over night, and counted the colonies that formed. This was attempted however Tryptic Soy Agar did not settle well enough for the sample to grow. In order to move forward, the equation provided by the correlation was used to determine the cell concentrations at the experimentally collected optical density values and plotted (*Figure 17* in *Appendix A*). Summary tables of calculations relating to *Figure 16* and *Figure 17* can be found in *Appendix B*. Multiple trials were performed to ensure data consistency. Some error was observed and will be discussed in a later section.

In order to observe the effects Filastatin has on the cell concentration of both *C. albicans* and *P. aeruginosa*, growth curves using 12.5 µM Filastatin and $3x10^4$ cells/ml were generated for a 24 hour period in Tryptic Soy Broth media. Optical density versus incubation time can be seen in *Figure 5* and *Figure 6* below. Due to a minimal amount of available Filastatin, one trial was conducted for each strain. Because of this adjustment, a control using just the fungus or bacteria

was grown simultaneously to ensure the strain was behaving similarly to the previous data. Summary tables of calculations relating to *Figure 5* and *Figure 6* can be found in *Appendix B.*

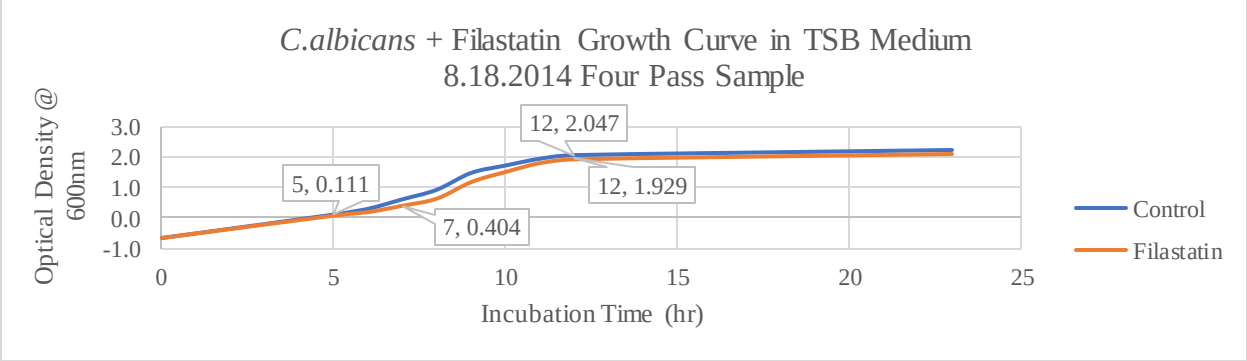

Figure 5: C. albicans + Filastatin Optical Density at 600nm vs. Incubation Time in hours

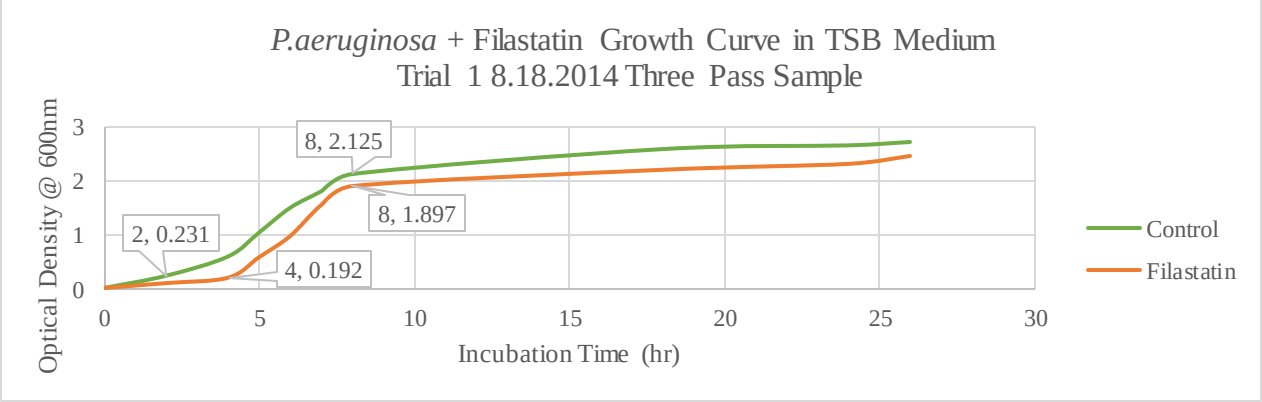

Figure 6: P. aeruginosa + Filastatin Optical Density at 600nm vs. Incubation Time in hours

Using the OD Cell Correlation Equation for *C. albicans* in *Figure 4* and the literature relationship of *P. aeruginosa* (Kim, 2012), cell concentrations per ml were calculated. These

results are illustrated in *Figure 7* and *Figure 8* below with summary tables of calculations in *Appendix B.*

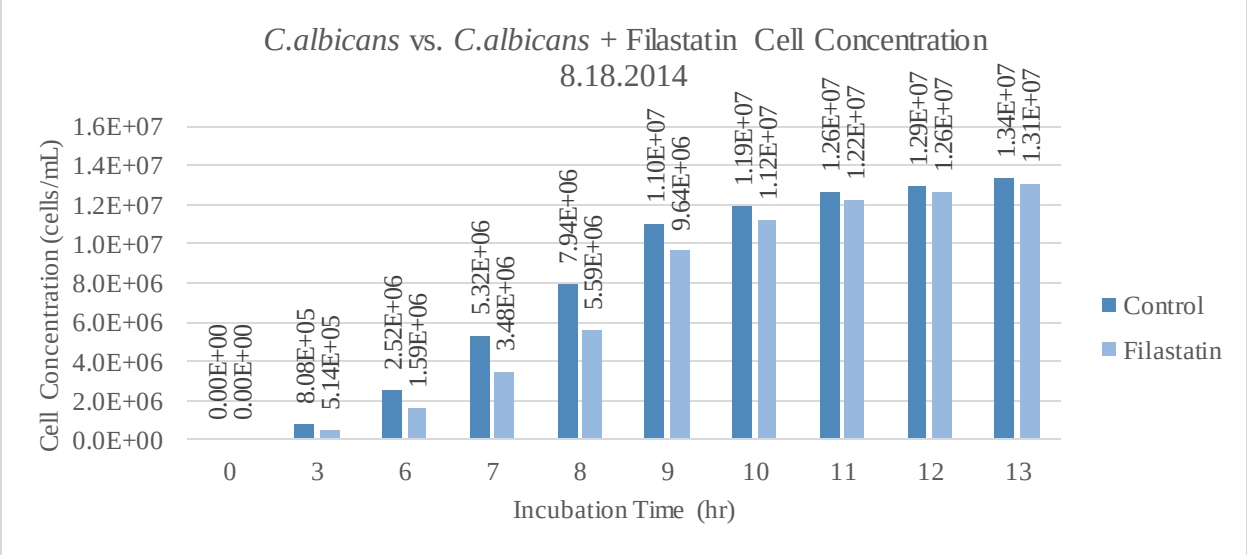

Figure 7: C. albicans vs. C. albicans + Filastatin Cell Concentration cells/ml

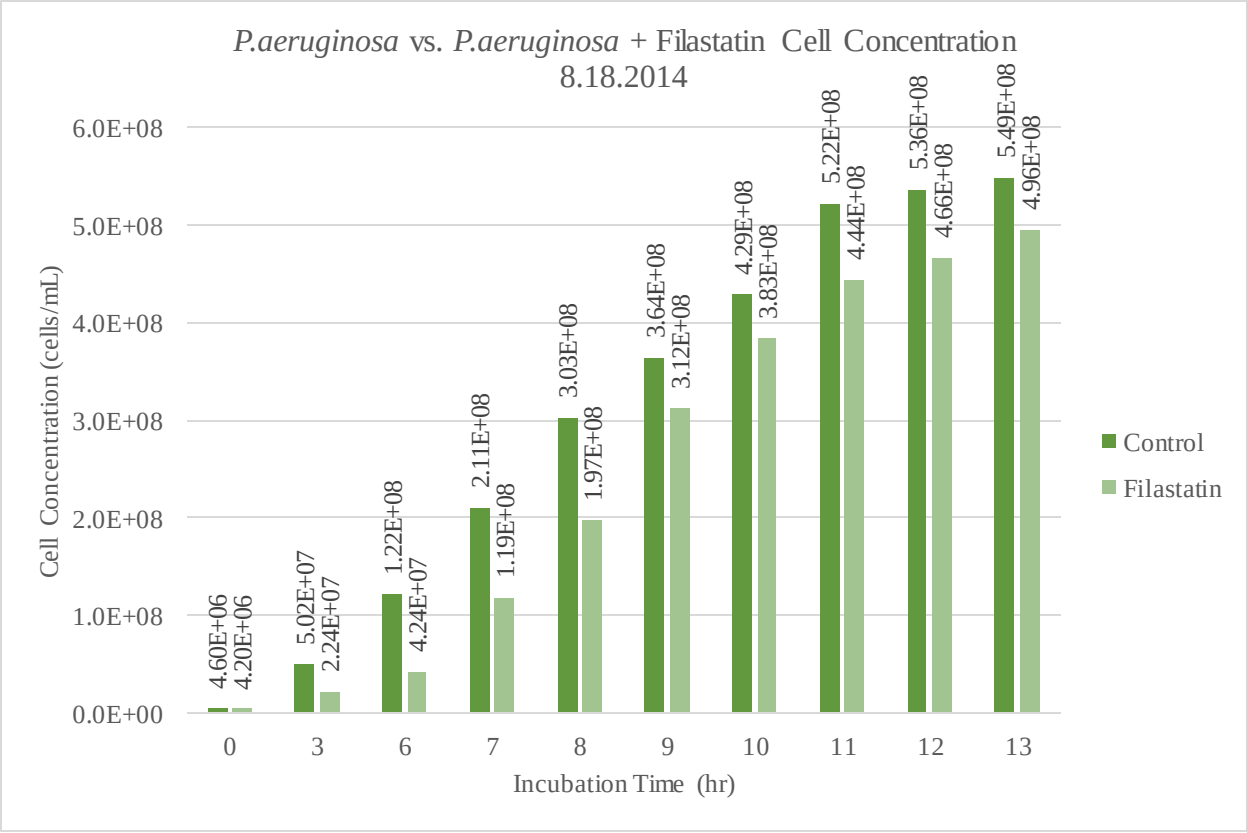

Figure 8: P. aeruginosa vs. P. aeruginosa + Filastatin Cell Concentration cells/ml

Quantitation of Biofilm Growth using Crystal Violet Adhesion Assay

To better understand biofilm formation of *C. albicans* and *P. aeruginosa*, biofilm growth experiments were conducted. These trials consisted of circulating $3*10^4$ cells/ml in 1L of TSB of either *C. albicans* or *P. aeruginosa* through a bioreactor containing 5 glass coupons under physiological flow. The coupons were either bare glass or coated with APTMS and placed in separate bioreactors. The experiments were run for about 17 hours to ensure that the fungus or bacteria completed all three growth phases established by the growth curve data. The glass coupons were then removed from the bioreactor and analyzed using the Crystal Violet Adhesion Assay outlined in *Materials and Methods*. Using Microsoft Excel 2013, OD values generated by the assay were tabulated and plotted against the coupon number (1 through 5 with 1 being at the inlet of the bioreactor). Due to the nature of the crystal violet stain, a threshold for OD was set at 0.05. Anything below this may be due to the buffer used to wash the coupons or any residual media. These plots can be seen in *Figure 18* and *Figure 19* in *Appendix A* along with average OD values in *Figure 9* and *Figure 10* below. Multiple trials were conducted to ensure data consistency. Summary tables of calculations relating to each figure can be seen in the *Appendix B*.

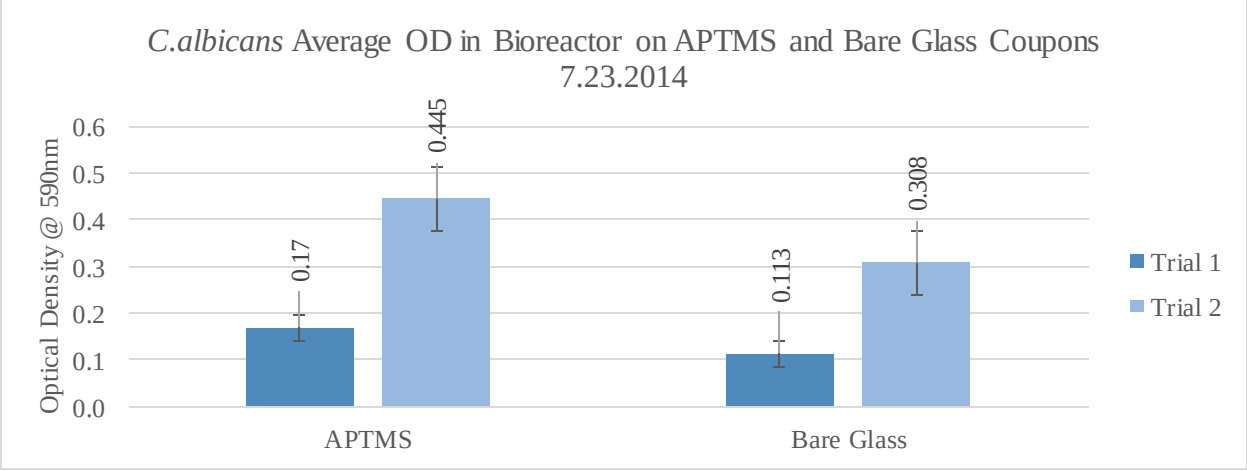

Figure 9: C. albicans Average Optical Density at 590nm in Bioreactor

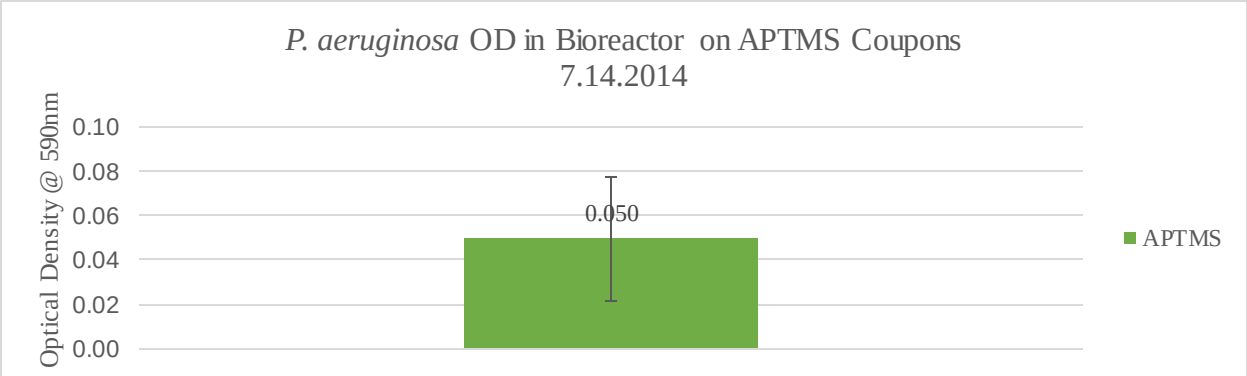

Figure 10: P. aeruginosa Average Optical Density at 590nm in Bioreactor

Using the previously determined OD vs. Cell Concentration correlation equations, cell concentration on each coupon was calculated. These values were plotted against the coupon number again as seen in *Figure 20* in *Appendix A* with average concentration values in *Figure 11*. Because the concentration of *P. aeruginosa* was mostly below the set baseline as seen in *Figure 9* cell concentration values were not calculated.

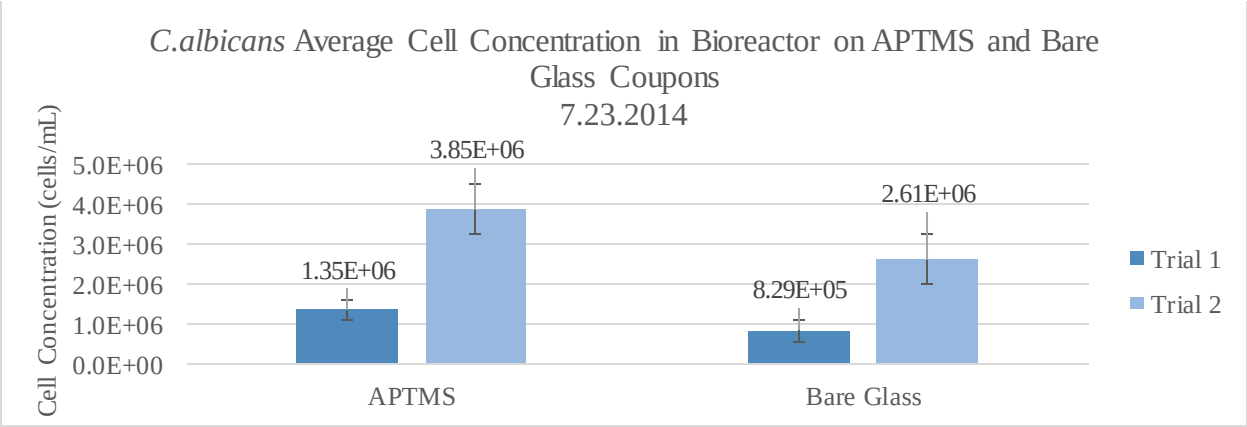

Figure 11: C. albicans Average Cell Concentration in cells/ml in Bioreactor

Morphology Analysis

To further investigate the effects Filastatin may have on *C. albicans*, a 200 µl sample of at its peak time was placed onto a hemacytometer during the growth curve with Filastatin (*Figure 5*).

As seen in *Figure 12* and *Figure 13* below, Filastatin has a huge effect on the morphological features of *C. albicans*.

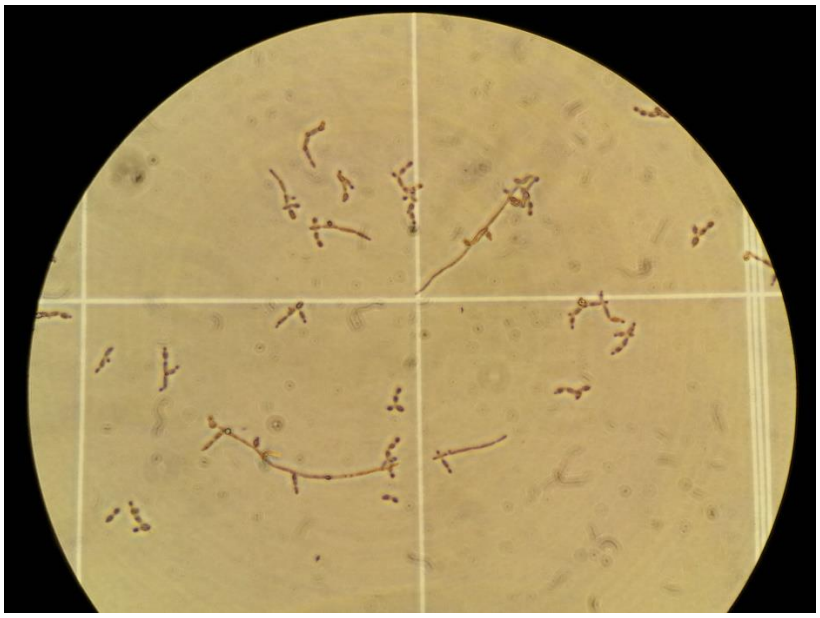

Figure 12: C. albicans at 12hrs in TSB

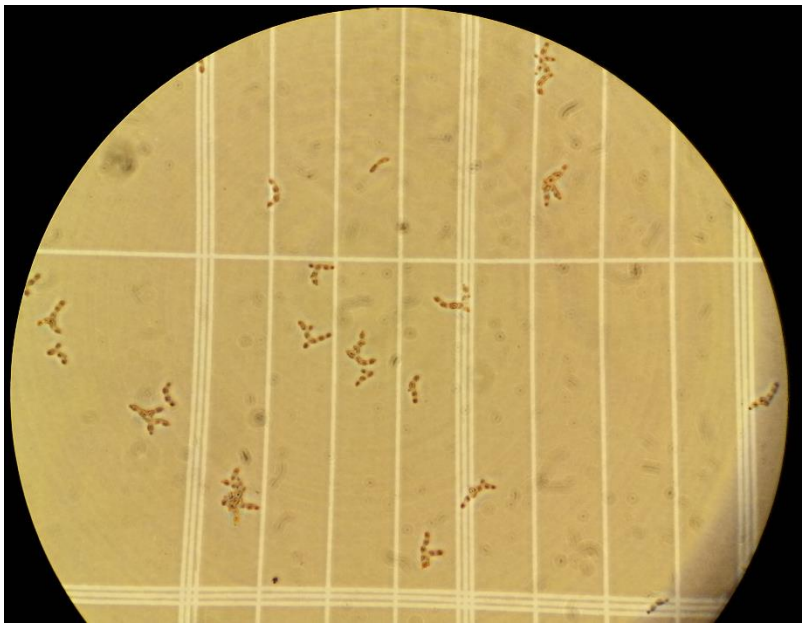

Figure 13: C. albicans + Filastatin at 12hrs in TSB

In *Figure 12*, the long infectious filament structure of *C. albicans* can be seen. This was expected as over time, *C. albicans* undergoes the structural transition from yeast to filament. In

Figure 13, no filament forms can be seen. This indicates that when Filastatin is grown with the fungus, *C. albicans* does not undergo the blastospore-filament transition known to induce virulence.

Discussion

The results of this project have shown that Filastatin does have an effect on the growth of both *Candida albicans* and *Pseudomonas aeruginosa*. As mentioned, bacteria and fungus possess different properties that give them unique infectious characteristics. *C. albicans* is an oval shaped fungus that undergoes phenotypic switching allowing for a rod shaped morphology to form. It is believed this hyphae filament form allows the fungus to penetrate and infect. When commensal, these hyphae rod forms are connected by oval nodes as seen in *Figure 1*. *P. aeruginosa* is a rod shaped bacterium with 1 polar flagellum as seen in *Figure 3* allowing it to move around and multiply quickly. As seen in the growth curve data, Filastatin shows some inhibitory effects on both *C. albicans* (*Figure 5*) and *P. aeruginosa* (*Figure 6*). *C. albicans* reaches a growth doubling time at about 5 hours normally as seen in *Figure 14* and *Figure 15****Error! Reference source not found.*** in *Appendix A*. When grown with 12.5 µM of Filastatin, this phase is not reached until 7 hours as labelled in *Figure 5*. *P. aeruginosa* reaches this growth doubling time much earlier at about 2 hours as seen in *Figure 16* and *Figure 17***.** When grown with 12.5 µM of Filastatin the same phase is reached about 2 hours later at 4 hours similarly to *C. albicans (Figure 6)*. As illustrated in *Figure 7* and *Figure 8*, Filastatin shows initial inhibitory effects but both the fungus and bacteria reach the same exponential doubling time eventually. This indicates that Filastatin does effect both *C. albicans* and *P. aeruginosa* in the desired way, inhibitory, but may not be a solution for elimination of the strain. Both *C. albicans* and *P. aeruginosa* appear to overcome the

Filastatin and eventually still grow to its full potential. Higher concentrations of Filastatin may be necessary to observe stronger inhibitory growth effects or no growth at all.

When reviewing the data from the crystal violet adhesion assay for biofilm formation, clear differences in the ability of *C. albicans* and *P. aeruginosa* to attach to the glass coupons was observed. APTMS prevents the adsorption of small organic molecules to the glass surface while increasing the number of bonds between them (Seed, 2003). Because of this a larger amount of biofilm was expected on the APTMS coated glass coupons and was observed in all results. *C. albicans* Biofilm formation appeared normal when performing the bioreactor experiments as seen in *Figure 18 and Figure 20*. Trial 1 OD and cell concentration values were much less than Trial 2. This was because the first trial used a strain directly thawed from the freezer, which may not have been 100% heathy fungus. The second trial used a strain grown in TSB for 24 hours first, making it a healthier sample in comparison. Average values were taken of optical density and cell concentration as seen in *Figure 9* and *Figure 11*. Standard deviation between the APTMS and Bare Glass coupons was calculated and added as error bars. The difference between APTMS and Bare Glass is very clear in these figures. Because APTMS binds more biofilm (Seed, 2003), bare glass coupons could be excluded for the remaining experiments. Bioreactor data for *P. aeruginosa* was inconclusive as seen in *Figure 19* and *Figure 10*. This is because the optical density of each coupon, with the exception of the first one, was below 0.05 making it below the set threshold. Such a small OD could be crystal violet binding to something other than bacteria or even just the stain resulting in a reading at 590nm. *P. aeruginosa* is a very small molecule in comparison to *C. albicans*. It most likely entered the bioreactor and exited without having an opportunity to settle onto a glass coupon. Decreasing the flow to increase the chances it has to settle on a coupon would lead to unrealistic results as simulating physiological flow to relate to bloodstream infections is

highly important. Increasing the initial concentration of *P. aeruginosa* is however an option as this could also increase the chances of cells attaching to the coupons and should be further explored.

Based on the results seen in *Figure 5*, *Figure 6*, *Figure 12*, and *Figure 13*, it can be concluded that Filastatin does inhibit the initial growth of *C. albicans* and *P. aeruginosa*. To further investigate the applications Filastatin can have on this fungus and bacteria, higher concentrations of the drug should be tested to determine if it simply delays the growth or can prevent it. If Filastatin is able to prevent the growth of both *C. albicans* and *P. aeruginosa*, it can be used to pre-treat medical devices or implants. Because Filastatin may be used to prevent infection within the body, a safe concentration for humans must also be determined.

Although the leading problem surrounding *C. albicans* and *P. aeruginosa* is medical related infections, Filastatin shows promising effects regarding biofilm formation of *C. albicans*. As observed, *C. albicans* is able to form a biofilm on glass coupons in a bioreactor. It was also identified that Filastatin inhibits the formation of filaments indicating that the pseudohyphae-hyphae transition that leads to infection may also be inhibited. Based on these conclusions Filastatin could be used as a mediator in many areas to prevent naturally occurring *C. albicans* from becoming infectious when forming biofilms on various surfaces, instruments, or implants. If Filastatin is proven to prevent growth when using higher concentrations, it may also prevent biofilm formation entirely and could be used as a pre-treatment for a variety of surfaces. These results bring us one step closer to understanding the effects Filastatin has on the growth of *C. albicans* and *P. aeruginosa*. With further exploration, Filastatin is even closer to implementation and decreasing the threatening statistics of medical related infections.

Bibliography

Centers for Disease Control and Prevention. *Antibiotic / Antimicrobial Resistance*. September 2013. June 2014. <http://www.cdc.gov/drugresistance/biggest_threats.html>.

Conly, J. M. "Where are all the new antibiotics? The new antibiotic paradox." *The Canadian Journal of Infectious Diseases and Medical Microbiology* (2005): 159-160. June 2014. <http://www.ncbi.nlm.nih.gov/pmc/articles/PMC2095020/#B12>.

Edens, W. "Tyrosine cross-linking of extracellular matrix is catalyzed by Duox, a multidomain oxidase/peroxidase with homology to the phagocyte oxidase subunit gp91phox." *The Journal of Cell Biology* 154.4 (2001): 879-892. June 2014. <http://jcb.rupress.org/content/154/4/879.long>.

Ernst, J. F. "Transcription factors in Candida albicans – environmental control of morphogenesis." *Journal of Microbiology* 146.8 (2000): 1763-1774. June 2014. <http://mic.sgmjournals.org/content/146/8/1763.long>.

Finkel, J. "GENETIC CONTROL OF CANDIDA ALBICANS BIOFILM DEVELOPMENT." *Nature Reviews Microbiology* 9.2 (2010): 109-118. June 2014. <http://www.ncbi.nlm.nih.gov/pmc/articles/PMC3891587/>.

Ganguly, Shantanu. "Mucosal biofilms of Candida albicans." *Current Opinion in Microbiology* 14.4 (2011): 380-385. June 2014. <http://www.ncbi.nlm.nih.gov/pmc/articles/PMC3159763/>.

Ivanov, Ivan E. "Relating the Physical Properties of Pseudomonas aeruginosa Lipopolysaccharides to Virulence by Atomic Force Microscopy." *Journal of Bacteriology* 193.5 (2010): 1259-1266. June 2014. <http://www.ncbi.nlm.nih.gov/pmc/articles/PMC3067594/#fn3>.

John Wiley and Sons. "Silanizing Glassware." Seed, Brian. *Current Protocols in Cell Biology*. John Wiley and Sons, 2003. June 2014. <http://onlinelibrary.wiley.com/doi/10.1002/0471143030.cba03es08/abstract;jsessionid=119AEBFC349FFFB911BEB34F14AED8E7.f03t02>.

Kadosh, David. "Induction of the Candida albicans Filamentous Growth Program by Relief of Transcriptional Repression: A Genome-wide Analysis." *Moleculer Biology of the Cell* 16.6 (2005): 2903-2912. June 2014. <http://www.ncbi.nlm.nih.gov/pmc/articles/PMC1142434/#ref52>.

Kang. "Pseudomonas aeruginosa Bacteremia: Risk Factors for Mortality and Influence of Delayed Receipt of Effective Antimicrobial Therapy on Clinical Outcome." *Clinical Infectious Diseases Oxford Journal* 37.6 (2003): 745-751. June 2014. <http://cid.oxfordjournals.org/content/37/6/745.long>.

Kim, Dong-ju. "Relation of microbial biomass to counting units for Pseudomonas aeruginosa." *African Journal of Microbiology Research* 6.21 (2012): 4620-4622. June 2014. <http://www.academicjournals.org/article/article1380721635_Kim%20et%20al.pdf>.

Kintz. "Regulation of lipopolysaccharide O antigen expression in Pseudomonas aeruginosa." *Future Microbiology* 3.2 (2008): 191-203. June 2014. <http://www.ncbi.nlm.nih.gov/pubmed/18366339/>.

Kojic. "Candida infections of medical devices." *Clinical Microbiology Review* 17.2 (2004): 255-267. June 2014. <http://www.ncbi.nlm.nih.gov/pubmed/15084500/>.

Liu, Haoping. "Co-regulation of pathogenesis with dimorphism and phenotypic switching in Candida albicans, a commensal and a pathogen." *International Journal of Medical Microbiology* 292.5 (2004): 299-311. June 2014. <http://www.sciencedirect.com/science/article/pii/S1438422104701095>.

Pier, GB. "Role of mutant CFTR in hypersusceptibility of cystic fibrosis patients to lung infections." *Science* 271.5245 (1996): 64-70. June 2014. <http://www.ncbi.nlm.nih.gov/pubmed/8539601/>.

Saville, S. P. "Engineered control of cell morphology in vivo reveals distinct roles for yeast and filamentous forms of Candida albicans during infection." *Eukaryot Cell* 2.5 (2003): 1053-1060. June 2014. <http://www.ncbi.nlm.nih.gov/pubmed/14555488/>.

Schaber, J. Andy. "Pseudomonas aeruginosa Forms Biofilms in Acute Infection Independent of Cell-to-Cell Signaling." *Infectious Immunology* 75.8 (2007): 3715-3721. June 2014. <http://www.ncbi.nlm.nih.gov/pmc/articles/PMC1952004/>.

Stanislavsky, ES. "Pseudomonas aeruginosa antigens as potential vaccines." *FEMS Microbiology Review* 21.3 (1997): 243-277. June 2014. <http://www.ncbi.nlm.nih.gov/pubmed/9451816>.

Tang, HB. "Contribution of specific Pseudomonas aeruginosa virulence factors to pathogenesis of pneumonia in a neonatal mouse model of infection." *Infectious Immunology* 64.1 (1996): 37-43. June 2014. <http://www.ncbi.nlm.nih.gov/pubmed/8557368/>.

Vitkauskienė, A. "Characteristics of carbapenem-resistant Pseudomonas aeruginosa strains in patients with ventilator-associated pneumonia in intensive care units." *Medicina (Kaunas)* 47.12 (2011): 652-660. June 2014. <http://www.ncbi.nlm.nih.gov/pubmed/22370463>.

www.hindawi.com. *Schematic overview of fungal biofilm resistance mechanisms*. n.d. <http://www.hindawi.com/journals/ijmicro/2012/528521/fig1/>.

Xie, Zhihong. "Candida albicans Biofilms Do Not Trigger Reactive Oxygen Species and Evade Neutrophil Killing." *The Journal of Infectious Diseases* 206.12 (2012): 1936-1945. June 2014. <http://jid.oxfordjournals.org/content/206/12/1936.full>.

Appendix A

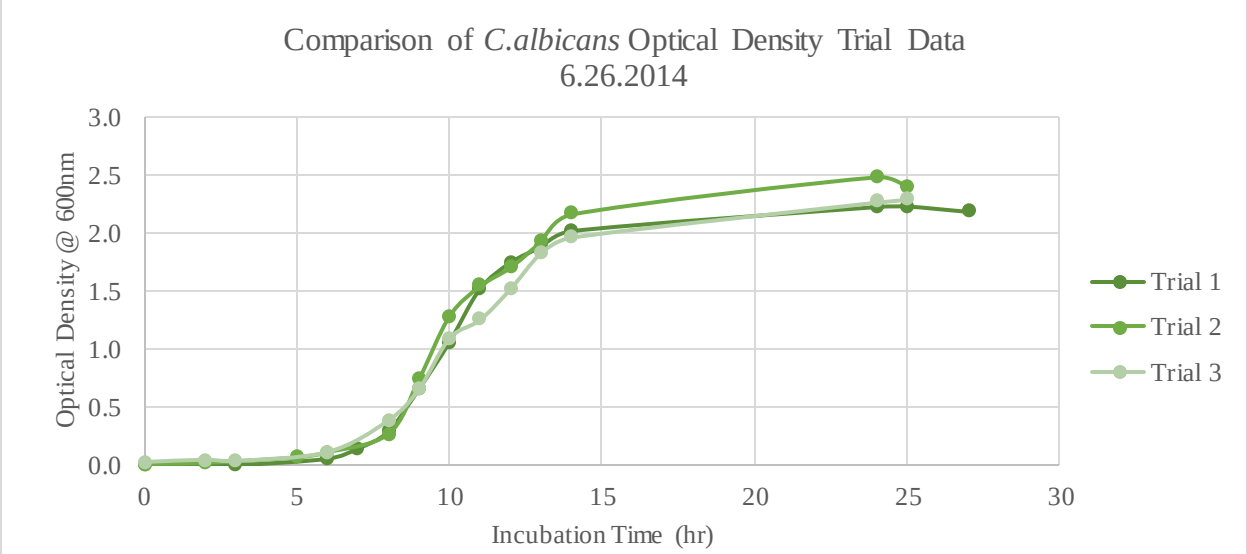

Figure 14: C. albicans OD at 600nm vs. Incubation Time in hours

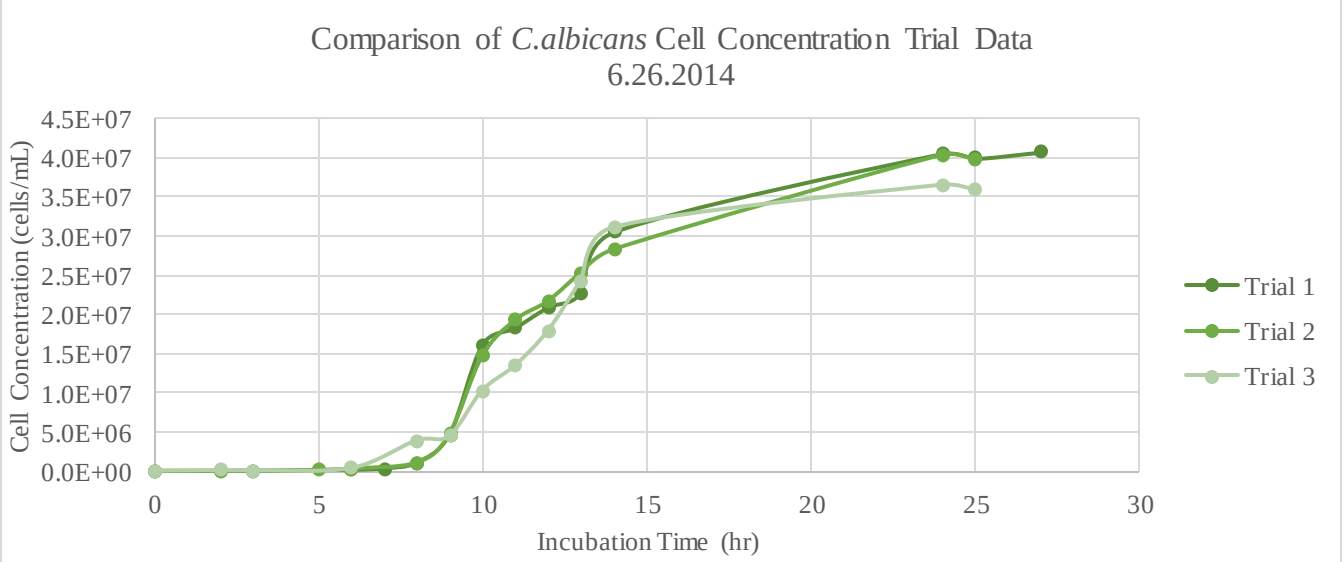

Figure 15: C. albicans Cell Concentration in cells/ml vs. Incubation Time in hours

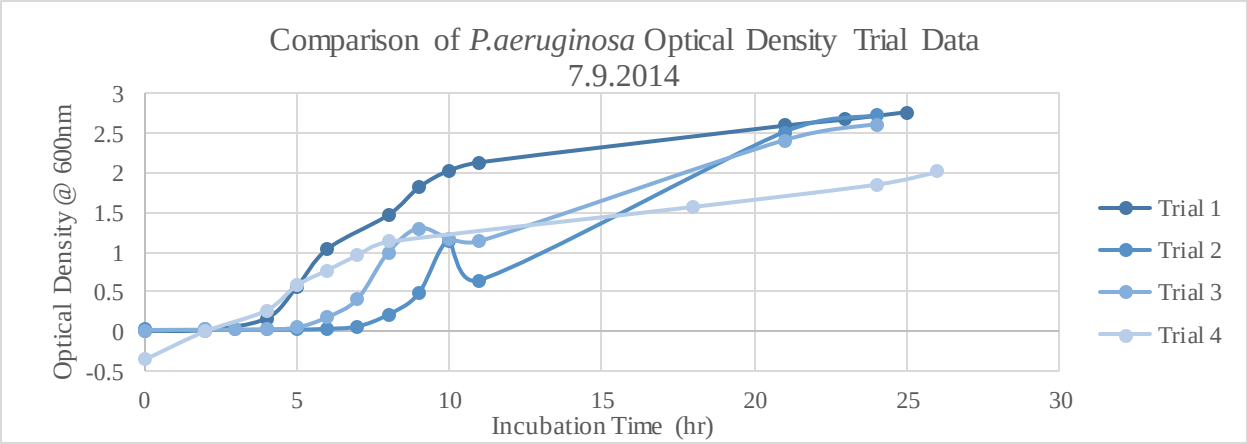

Figure 16: P. aeruginosa OD at 600nm vs. Incubation Time in hours

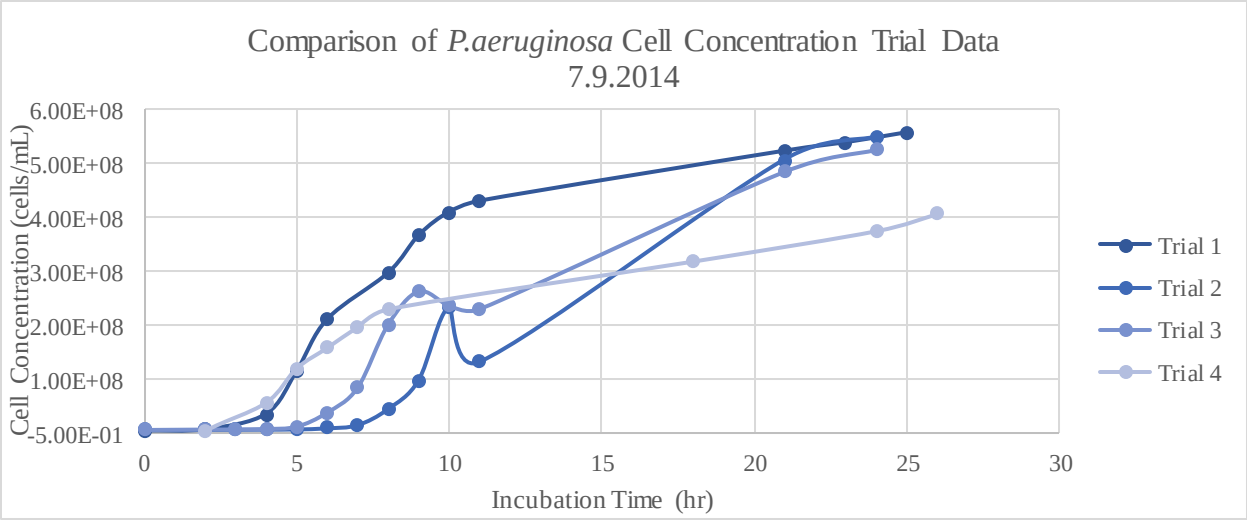

Figure 17: P. aeruginosa Cell Concentration in cells/ml vs. Incubation Time in hours

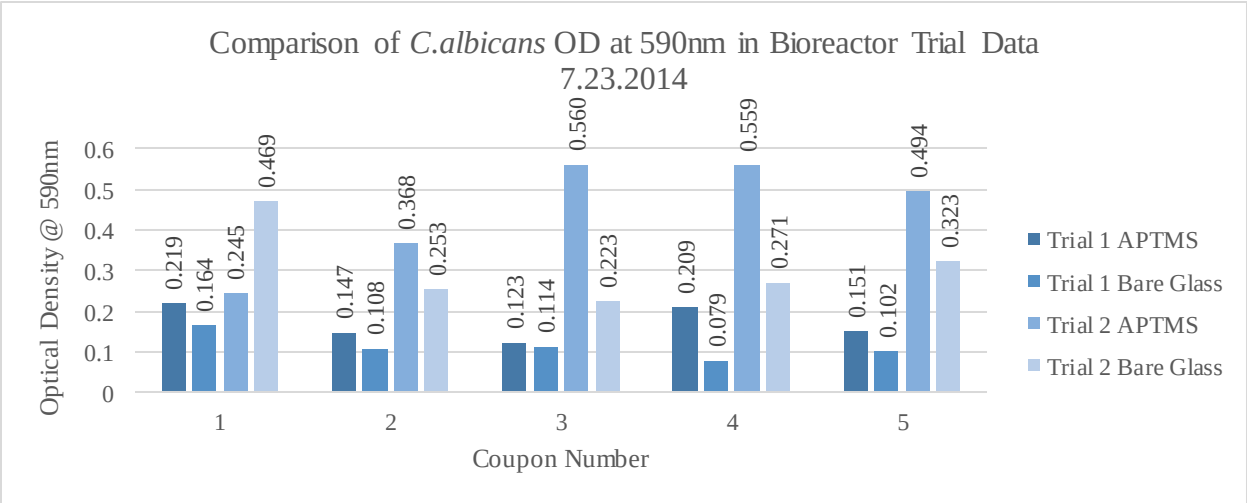

Figure 18: C. albicans Optical Density at 590nm vs. Coupon Number in Bioreactor

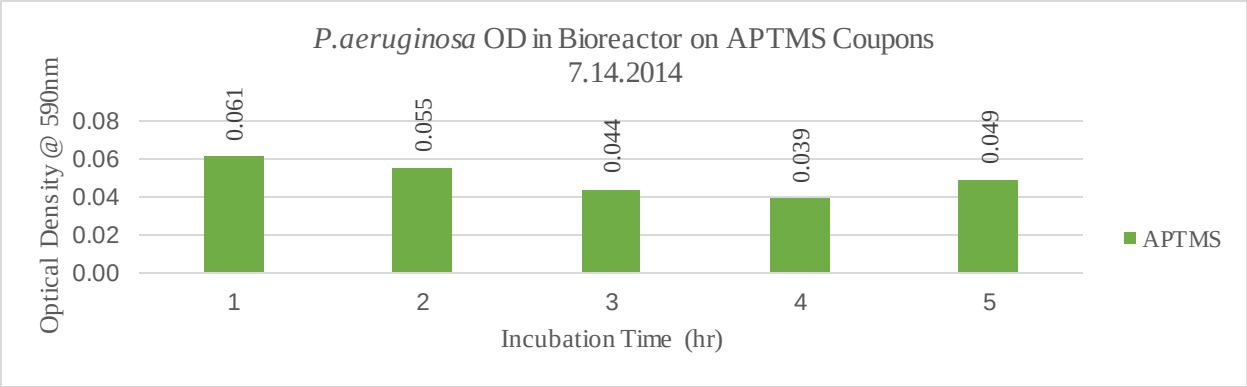

Figure 19: P. aeruginosa Optical Density at 590nm vs. Coupon Number in Bioreactor

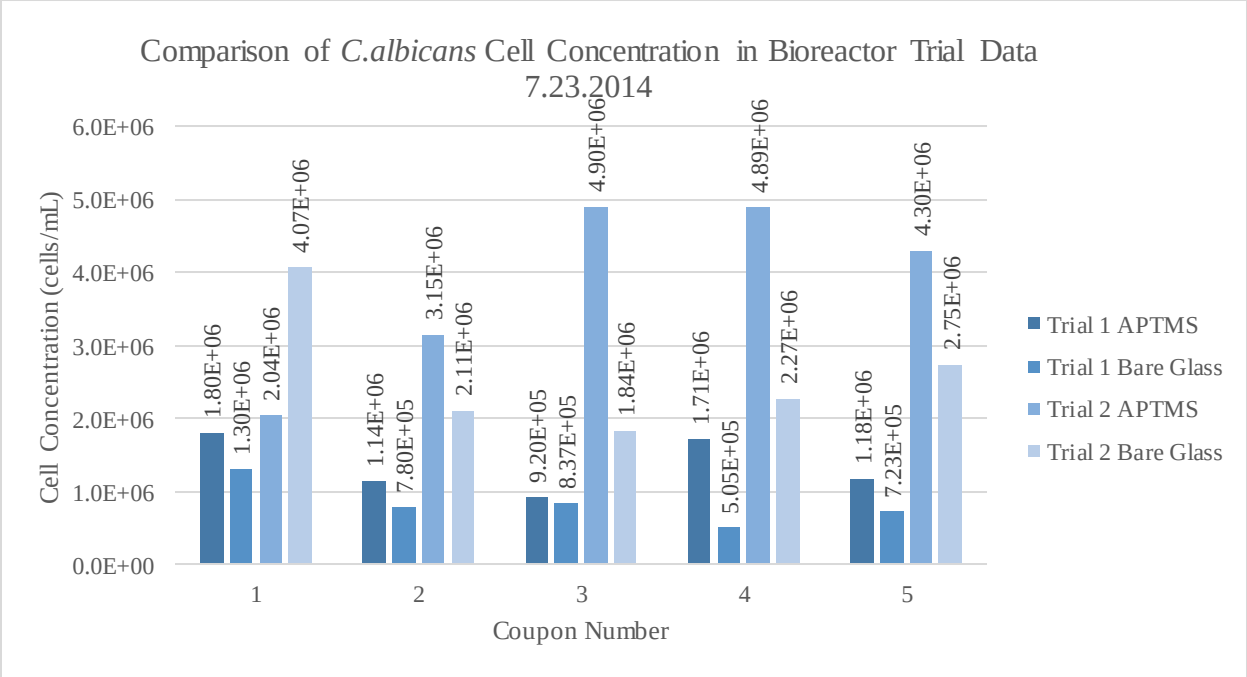

Figure 20: C. albicans Cell Concentration in cells/ml vs. Coupon Number in Bioreactor

Appendix B

Figure 14 Related:

***C. albicans* Trial 1 Growth Curve 5.23.2014**	
Incubation Time (hr)	**OD Reading (600nm)**
0	0.000
3	0.000
6	0.053
7	0.140
8	0.287

9	0.650
10	1.053
11	1.513
12	1.742
13	1.878
14	2.015
24	2.223
25	2.228
27	2.182
***C. albicans* Trial 2 Growth Curve 6.4.2014**	
Incubation Time (hr)	**OD Reading (600nm)**
0	0.000
2	0.010
5	0.057
6	0.101
8	0.260
9	0.734
10	1.280
11	1.540
12	1.702
13	1.927
14	2.162
24	2.485
25	2.396
***C. albicans* Trial 3 Growth Curve 6.26.2014**	
Incubation Time (hr)	**OD Reading (600nm)**
0	0.015
2	0.035
3	0.025
6	0.101
8	0.376
9	0.648
10	1.088
11	1.248
12	1.517
13	1.827
14	1.962
24	2.266
25	2.289

Figure 15 Related:

***C .albicans* Cell Counting using Trial 1 Sample 5.23.2014**				
Incubation Time (hr)	**Cell Count**	**Average #cells/square**	**Dilution Factor**	**Concentration (cells/mL)**
0	0	0	1	0.000E+00
3	5	1	1	1.000E+04
6	71	14.2	1	1.420E+05
7	158	31.6	1	3.160E+05
8	526	105.2	1	1.052E+06
9	229	45.8	10	4.580E+06
10	80	16	100	1.600E+07
11	91	18.2	100	1.820E+07
12	104	20.8	100	2.080E+07
13	113	22.6	100	2.260E+07
14	152	30.4	100	3.040E+07
24	202	40.4	100	4.040E+07
25	199	39.8	100	3.980E+07
27	203	40.6	100	4.060E+07
***C. albicans* Cell Counting using Trial 2 Sample 6.4.2014**				
Incubation Time (hr)	**Cell Count**	**Average #cells/square**	**Dilution Factor**	**Concentration (cells/mL)**
0	0	0	1	0.000E+00
2	4	0.8	1	8.000E+03
5	69	13.8	1	1.380E+05
6	156	31.2	1	3.120E+05
8	531	106.2	1	1.062E+06
9	233	46.6	10	4.660E+06
10	73	14.6	100	1.460E+07
11	96	19.2	100	1.920E+07
12	108	21.6	100	2.160E+07
13	126	25.2	100	2.520E+07
14	141	28.2	100	2.820E+07
24	201	40.2	100	4.020E+07
25	198	39.6	100	3.960E+07
***C. albicans* Cell Counting using Trial 3 Sample 6.26.2014**				
Incubation Time (hr)	**Cell Count**	**Average #cells/square**	**Dilution Factor**	**Concentration (cells/mL)**
0	6	1.2	1	1.200E+04
2	38	7.6	1	7.600E+04
3	32	6.4	1	6.400E+04
6	167	33.4	1	3.340E+05
8	193	38.6	10	3.860E+06

9	222	44.4	10	4.440E+06
10	51	10.2	100	1.020E+07
11	67	13.4	100	1.340E+07
12	89	17.8	100	1.780E+07
13	121	24.2	100	2.420E+07
14	155	31	100	3.100E+07
24	182	36.4	100	3.640E+07
25	179	35.8	100	3.580E+07

Figure 16 Related:

***P. aeruginosa* Trial 1 Growth Curve 6.4.2014**	
Incubation Time (hr)	**OD Reading (600nm)**
0	0.001
2	0.013
4	0.157
5	0.556
6	1.035
8	1.466
9	1.815
10	2.03
11	2.131
21	2.595
23	2.673
25	2.766

***P. aeruginosa* Trial 2 Growth Curve 6.26.2014**	
Incubation Time (hr)	**OD Reading (600nm)**
0	0.018
2	0.019
3	0.020
4	0.021
5	0.023
6	0.033
7	0.062
8	0.210
9	0.475
10	1.146
11	0.646
21	2.513
24	2.722

P. aeruginosa Trial 3 Growth Curve 6.26.2014	
Incubation Time (hr)	**OD Reading (600nm)**
0	0.015
2	0.018
3	0.020
4	0.024
5	0.045
6	0.175
7	0.405
8	0.990
9	1.299
10	1.170
11	1.135
21	2.408
24	2.611

P. aeruginosa Trial 4 Growth Curve 7.3.2014	
Incubation Time (hr)	**OD Reading (600nm)**
0	-0.359
2	0.001
4	0.265
5	0.583
6	0.773
7	0.966
8	1.132
18	1.575
24	1.857
26	2.016

Figure 17 Related:

P. aeruginosa Cell Concentration OD Correlation	
using equation y = 2E+8x+4E+6	
Optical Density (600nm)	**Cell Concentration (cell/mL)**
0.0	4.00E+06
0.2	4.40E+07
0.4	8.40E+07
0.6	1.24E+08
0.8	1.64E+08
1.0	2.04E+08

1.2	2.44E+08
1.4	2.84E+08
1.6	3.24E+08
1.8	3.64E+08
2	4.04E+08
2.2	4.44E+08
2.4	4.84E+08
2.6	5.24E+08

***P.aeruginosa* Cell Counting using Trial 1 Sample & y = 2E+8x+4E+6**		
Incubation Time (hr)	**Optical Density (600nm)**	**Concentration (cells/mL)**
0	0.001	4.20E+06
2	0.013	6.60E+06
4	0.157	3.54E+07
5	0.556	1.15E+08
6	1.035	2.11E+08
8	1.466	2.97E+08
9	1.815	3.67E+08
10	2.03	4.10E+08
11	2.131	4.30E+08
21	2.595	5.23E+08
23	2.673	5.39E+08
25	2.766	5.57E+08

***P.aeruginosa* Cell Counting using Trial 2 Sample & y = 2E+8x+4E+6**		
Incubation Time (hr)	**Optical Density (600nm)**	**Concentration (cells/mL)**
0	0.018	7.60E+06
2	0.019	7.80E+06
3	0.020	8.00E+06
4	0.021	8.20E+06
5	0.023	8.60E+06
6	0.033	1.06E+07
7	0.062	1.64E+07
8	0.210	4.60E+07
9	0.475	9.90E+07
10	1.146	2.33E+08
11	0.646	1.33E+08
21	2.513	5.07E+08
24	2.722	5.48E+08

P.aeruginosa Cell Counting using Trial 3 Sample & y = 2E+8x+4E+6		
Incubation Time (hr)	**Optical Density (600nm)**	**Concentration (cells/mL)**
0	0.015	7.00E+06
2	0.018	7.60E+06
3	0.020	8.00E+06
4	0.024	8.80E+06
5	0.045	1.30E+07
6	0.175	3.90E+07
7	0.405	8.50E+07
8	0.990	2.02E+08
9	1.299	2.64E+08
10	1.170	2.38E+08
11	1.135	2.31E+08
21	2.408	4.86E+08
24	2.611	5.26E+08

P.aeruginosa Cell Counting using Trial 4 Sample & y = 2E+8x+4E+6		
Incubation Time (hr)	**Optical Density (600nm)**	**Concentration (cells/mL)**
0	-0.359	-6.78E+07
2	0.001	4.20E+06
4	0.265	5.70E+07
5	0.583	1.21E+08
6	0.773	1.59E+08
7	0.966	1.97E+08
8	1.132	2.30E+08
18	1.575	3.19E+08
24	1.857	3.75E+08
26	2.016	4.07E+08

Figure 5 Related:

C. albicans + Filastatin Trial 1 Growth Curve 8.18.2014				
Incubation Time (hr)	**OD Reading Control (600nm)**	**OD Reading (600nm)**	**Cell Concentration Control**	**Cell Concentration**
0	-0.653	-0.655	0.00E+00	0.00E+00
5	0.111	0.080	8.08E+05	5.14E+05
6	0.298	0.196	2.52E+06	1.59E+06
7	0.607	0.404	5.32E+06	3.48E+06
8	0.919	0.637	7.94E+06	5.59E+06
9	1.467	1.180	1.10E+07	9.64E+06
10	1.708	1.514	1.19E+07	1.12E+07

11	1.929	1.804	1.26E+07	1.22E+07
12	2.047	1.929	1.29E+07	1.26E+07
23	2.214	2.105	1.34E+07	1.31E+07

Figure 6 Related:

***P. aeruginosa* + Filastatin Trial 1 Growth Curve 8.18.2014**				
Incubation Time (hr)	**OD Reading Control (600nm)**	**OD Reading (600nm)**	**Cell Concentration Control**	**Cell Concentration**
0	0.003	0.001	4.60E+06	4.20E+06
2	0.231	0.092	5.02E+07	2.24E+07
4	0.589	0.192	1.22E+08	4.24E+07
5	1.035	0.573	2.11E+08	1.19E+08
6	1.495	0.965	3.03E+08	1.97E+08
7	1.802	1.541	3.64E+08	3.12E+08
8	2.125	1.897	4.29E+08	3.83E+08
18	2.59	2.201	5.22E+08	4.44E+08
24	2.66	2.311	5.36E+08	4.66E+08
26	2.723	2.458	5.49E+08	4.96E+08

Figure 7 Related:

See Figure 5 Related

Figure 8 Related:

See Figure 6 Related

Figure 17 Related:

Trial 1 Glass Coupon Bioreactor 5.23.2014				
3E4 329µl/min for 17hrs @ 37°C				
Surface	**Surface Position**	**Well Number**	**OD Reading (590nm)**	**Cell Concentration**
APTMS Glass Coupon	1	1A	0.219	1.80E+06
APTMS Glass Coupon	2	2A	0.147	1.14E+06
APTMS Glass Coupon	3	3A	0.123	9.20E+05
APTMS Glass Coupon	4	4A	0.209	1.71E+06
APTMS Glass Coupon	5	5A	0.151	1.18E+06
Bare Glass Coupon	1	1B	0.164	1.30E+06
Bare Glass Coupon	2	2B	0.108	7.80E+05

Bare Glass Coupon	3	3B	0.114	8.37E+05
Bare Glass Coupon	4	4B	0.079	5.05E+05
Bare Glass Coupon	5	5B	0.102	7.23E+05

Trial 2 Glass Coupon Bioreactor 7.23.2014				
3E4 329µl/min for 17hrs @ 37°C				
Surface	**Surface Position**	**Well Number**	**OD Reading (590nm)**	**Cell Concentration**
APTMS Glass Coupon	1	1A	0.245	2.04E+06
APTMS Glass Coupon	2	2A	0.368	3.15E+06
APTMS Glass Coupon	3	3A	0.560	4.90E+06
APTMS Glass Coupon	4	4A	0.559	4.89E+06
APTMS Glass Coupon	5	5A	0.494	4.30E+06
Bare Glass Coupon	1	1B	0.469	4.07E+06
Bare Glass Coupon	2	2B	0.253	2.11E+06
Bare Glass Coupon	3	3B	0.223	1.84E+06
Bare Glass Coupon	4	4B	0.271	2.27E+06
Bare Glass Coupon	5	5B	0.323	2.75E+06

Figure 9 Related:

Average OD Bioreactor Trial Data Comparison		
Trial	**1**	**2**
APTMS	0.17	0.445
Bare Glass	0.113	0.308

Figure 19 Related:

Trial 1 Bioreactor (estimated cell count) 7.14.2014			
3E5 329µl/min for 17hrs @ 37°C			
Surface	**Surface Position**	**Well Number**	**OD Reading (590nm)**
APTMS Glass Coupon	1	1A	0.061
APTMS Glass Coupon	2	2A	0.055
APTMS Glass Coupon	3	3A	0.044
APTMS Glass Coupon	4	4A	0.039
APTMS Glass Coupon	5	5A	0.049
Bare Glass Coupon	1	1B	NA

Bare Glass Coupon	2	2B	NA
Bare Glass Coupon	3	3B	NA
Bare Glass Coupon	4	4B	NA
Bare Glass Coupon	5	5B	NA

Figure 10 Related:

Average OD Trial 1 Bioreactor	
Mean APTMS	0.050

Figure 11 Related:

Average Cell Concentration Bioreactor Trial Data Comparison		
Trial	**1**	**2**
APTMS	1.35E+06	3.85E+06
Bare Glass	8.29E+05	2.61E+06
Standard Deviation	261660	623400